

METHODS TO RECOVER THE NARROW DICKE SUB-DOPPLER FEATURE  
IN EVACUATED WALL-COATED CELLS WITHOUT RESTRICTIONS ON CELL SIZE

H. G. Robinson  
Duke University  
Durham, North Carolina 27706

ABSTRACT

The hyperfine resonance observed in evacuated wall-coated cells with dimensions  $< \lambda/2$  ( $\lambda$  is the hyperfine resonance wavelength) consists of a narrow Dicke sub-Doppler linewidth feature, the 'spike', superimposed on a broad pedestal. The hydrogen maser provides a classic example of this lineshape. As cell size is increased, an effect unique to evacuated wall-coated cells occurs. Certain combinations of microwave field distribution and cell size result in a lineshape having a pedestal with a small spike feature or only the broad pedestal with no spike. Such conditions are not appropriate for atomic frequency standard applications. This paper reviews the cause of the evacuated wall-coated cell lineshape and discusses methods to recover the narrow spike feature without restrictions on cell size. One example will be a cell with dimensions having equal volumes of exposure to opposite phases of the microwave magnetic field. The typical signal recovery technique would have no spike in this case. Potential application is especially appropriate for Rb or Cs evacuated wall-coated cells.

INTRODUCTION

The hydrogen maser provides a practical example of the use of the evacuated wall-coated cell in an atomic clock application. The high Q, narrow line width, homogeneous lineshape afforded by this technique provides one of technology's best clocks. In this use, the cell is designed to have dimensions  $< \lambda(H)/2$  where  $\lambda$  is the cavity wavelength of the hyperfine transition (free-space  $\lambda \sim 21$  cm). The recent demonstration [1-3] of narrow,  $^{87}\text{Rb}$  hyperfine transitions in an evacuated wall-coated sealed cell (EWSC) raises the possibility of taking advantage of the homogeneous lineshape for a superior  $^{87}\text{Rb}$  atomic frequency standard. Here the free-space wavelength,  $\lambda \sim 4.4$  cm, is considerably smaller than that for hydrogen. Thus relatively small Rb cells compared to those used for hydrogen still may have dimensions  $> \lambda(\text{Rb})/2$ . In addition, both hyperfine resonance linewidth and wall shift are inversely proportional to the cell size: signal is proportional to cell size. Such considerations alone would lead to use of larger cells for improvement in these important parameters.

The understanding of the effects of cell size on lineshape then becomes an important design consideration. In this paper, we review the basic cause of the EWSC lineshape with a simple one-dimensional model and discuss techniques to take advantage of the large relaxation times available in such cells even if cell dimensions are  $> \lambda/2$ .

DISCUSSION

A number of theoretical treatments have been made which address the

lineshape of motionally averaging systems. Dicke's is well-known for the Doppler-linewidth reduction as applied to an atom diffusing in an inert buffer gas.[4] The theory for the hydrogen maser lineshape was particularly applicable to cells with dimensions  $< \lambda/2$  where only a small microwave phase variation exists across the cell.[5] A theoretical statistical treatment of the lineshape for TE111 and TE011 mode cavities has been made with some simplifying assumptions.[6] A two-dimensional model Monte Carlo trajectory calculation has given results for both wall-coated and gas filled cells.[7] Three dimensional Monte Carlo trajectory calculations have been used to explore the lineshape of a Zeeman transition in the spherical evacuated wall-coated cell in the presence of magnetic field inhomogeneities.[8] Experiment and theory were compared with good agreement. The code developed was later employed in studies on systematic effects of magnetic field gradients on the hydrogen maser.[9]. The reader will find these papers informative.

The lineshape characteristic of the evacuated wall-coated cell is a narrow sub-Doppler spike centered on a broad pedestal having approximately the full Doppler width ( $\sim 9\text{kHz}$ ) of the hyperfine transition . The width of the spike is limited by the relaxation time of the atom-wall interaction. The narrowest width attained for  $^{87}\text{Rb}$  has been  $\sim 10\text{Hz}$  FWHM -- the observed lineshape was Lorentzian.[1] The interest in this paper is in understanding basic phenomena of the averaging process leading to the relative heights of the spike and pedestal in order to maximize the former and minimize the latter. This not only moves the signal toward an optimum but also minimizes systematic effects associated with the pedestal.

First we recall Dicke's one-dimensional model. A radiating oscillator is permitted to bounce between two confining walls. The moving oscillator as seen in the laboratory frame emits a constant amplitude, square-wave frequency modulated wave. Thus the oscillator is periodically Doppler-shifted either up or down from the resting oscillator's frequency due to its rattling motion. The resulting frequency spectrum is found by Fourier analyzing the time-dependent oscillation frequency. The result is the 'lineshape' for the motionally averaged radiating system.

The simple model chosen for discussion in the case of the evacuated wall-coated cell is very similar to Dicke's. It consists of an ensemble able to move in one-dimension in an evacuated cell with walls which permit bouncing without perturbing the quantum state. A given atom is acted on by a standing-wave field applied to cause a transition from one hyperfine state to another [e.g.  $(2,0) \leftrightarrow (1,0)$ ]. In the frame of the atom, an oscillating field is seen which is amplitude modulated due to motion through the standing-wave field. Two special cases are considered: in the first, the cell has dimension  $D = \lambda/2$ .



The first sketch shows the cell with atom moving to right with speed  $v$  in the standing-wave field. After collision with the right-hand wall, the atom

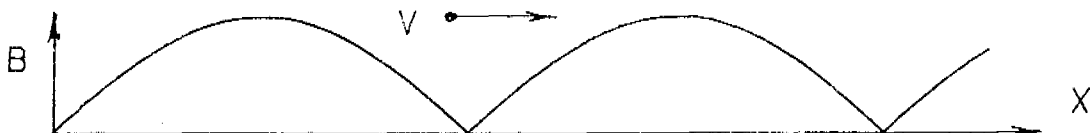
moves with the same speed to the left through the same standing field. The field  $B_1(x)$  seen by the atom at position  $x$  is

$$B_1(x) = \sin \frac{2\pi x}{\lambda} \cos \omega_0 t = \sin \frac{2\pi v t}{\lambda} \cos \omega_0 t = \sin \omega_D t \cos \omega_0 t : 0 < t < T/2$$

$$= \sin \frac{2\pi v(T-t)}{\lambda} \cos \omega_0 t = \sin \omega_D(T-t) \cos \omega_0 t : T/2 < t < T$$

where  $\omega_D = 2\pi v/\lambda$ .

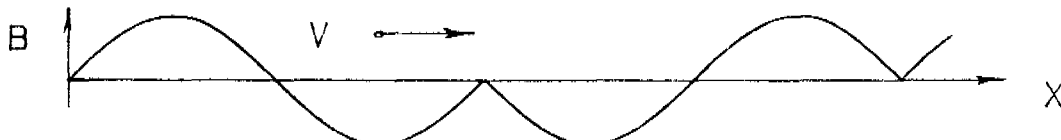
Apparently this system can be replaced by one in which the atom moves only to the right in the field amplitude arranged to mimic that actually seen by the atom. See sketch below. Fourier analysis of the periodic waveform  $B_1(x)$  gives the frequency spectrum seen by the atom.



This spectrum consists of symmetric sidebands on either side of the applied frequency  $\omega_0$  and a central non-shifted component at  $\omega_0$ . Fourier analysis gives this central amplitude simply as  $\langle B_1(x) \rangle$ , the spatial average of the field over the cell. The transition probability, proportional to the square of this perturbation, gives a spike signal proportional to  $\langle B_1 \rangle^2$ .

The presence of well-defined sidebands is an artifact of the assumption of a constant speed for a given member of the ensemble. A non-coherent superposition of signals from an ensemble with a Maxwell-Boltzmann distribution of speeds produces the pedestal-spike lineshape. The pedestal height is taken proportional to  $\langle B_1^2 \rangle$  as a result of the incoherent addition of sidebands. Note that the width of the pedestal is expected to be related to that of the non-narrowed Doppler width. Other considerations are involved in attaining the relative heights of the spike and pedestal signals, e.g., the linewidths of the respective features. This will be discussed shortly. No doubt our assumptions are too simplified -- but some of the basic physics generating the lineshape becomes clearer.

The second case treated in the same spirit is that of a cell with  $D = \lambda$ . The equivalent periodic field seen by an atom traveling always to the right is sketched below.



Fourier analysis of this periodic waveform obviously will give  $\langle B_1(x) \rangle = 0$  since the average value of the waveform is zero by symmetry. Thus no spike would be seen under these conditions of excitation no matter how strong the applied  $B_1$  is. However the broad pedestal with its characteristic Doppler width will appear since  $\langle B_1^2 \rangle$  is not zero.

Another explanation for the absence of the spike follows by considering an arbitrary atom which begins a transition from state 1 to state 2 under stimulation of the oscillating microwave magnetic field. Since the atom is not constrained to remain fixed in space, it moves through the cell bouncing from wall to wall in straight line paths. As long as it moves through a region of the cell having the same spatial phase as it experienced at the beginning of its transition, it will continue making the transition from state 1 to state 2. However, when it crosses a microwave spatial phase boundary and finds itself in a region of the cell having the opposite spatial phase from that which it first experienced, the transition process will reverse and move from 2 back to state 1. On the average then, it is possible for the atoms bouncing from the walls of the cell to have a net zero transition probability for the spike component of the lineshape.

Thus even with a more detailed theory of the motionally averaged lineshape in evacuated wall-coated cells, we know what conditions will maximize the spike. In the limit of no microwave saturation, the transition probability for the spike is found by considering the case of a  $\delta$ -function of stimulating radiation interacting with a Lorentzian lineshape of width  $\delta\nu$ <sub>spike</sub>. Thus the spike height will be proportional to  $\langle B_1 \rangle^2 / \delta\nu$ <sub>spike</sub>. On the other hand, the transition probability for the pedestal requires a broad stimulating spectral width interacting with a narrow intrinsic Lorentzian lineshape. The pedestal height then is proportional to the energy density in the field per unit frequency,  $\propto \langle B_1 \rangle / \delta\nu$ <sub>ped</sub>. Therefore the ratio of heights  $S_s/S_p$  will be proportional to

$$\frac{S_s}{S_p} \propto \frac{\langle B_1 \rangle^2 \times \delta\nu_p}{\langle B_1 \rangle^2 \times \delta\nu_s}$$

The  $\delta\nu$ <sub>s</sub> are the spike and pedestal linewidths. The spike linewidth is a delta-function in the one-dimensional model — there is zero Doppler shift and zero Doppler width. In a real cell, the intrinsic linewidth is then determined principally by the actual wall-relaxation mechanism which is limited mainly by dispersion in the phase shift due to the atom-wall interaction.

The three dimensional Monte Carlo calculations[8] clearly showed that the atom statistically prefers to bounce 'back and forth' revisiting the region from which it came before the last wall bounce. This is a consequence of the boundary condition that  $\underline{R} \cdot \underline{v} < 0$  where  $\underline{R}$  is the vector from the cell center to the moving atom and  $\underline{v}$  is the atom's velocity. The wall allows access only to a  $2\pi$  solid angle after a collision while in an atom-gas collision, access to  $4\pi$  solid angle is available. These physical constraints separate atom-wall collisions in evacuated cells from atom-gas collisions in gas cells. Thus one can expect different consequences to follow from collisions in wall-coated evacuated cells and those in gas cells.[10] Motional averaging effects are dramatically different.

An important issue regarding possible use of the EWSC in atomic frequency standards is the attainable figure of merit,  $M$  (signal-to-noise/linewidth), relative to that, say, of the Rb gas cell device. Consider a Lorentzian line with width 500Hz and height  $S_o$  attained in a cell with Rb density  $p_o$ . Thus  $M \propto S_o / 500$ . If it were possible to reduce linewidth by a factor of 10 at constant Rb density, the height of the resonance would increase to  $10S_o$ . [Since the spike has a Lorentzian lineshape to a good approximation, the

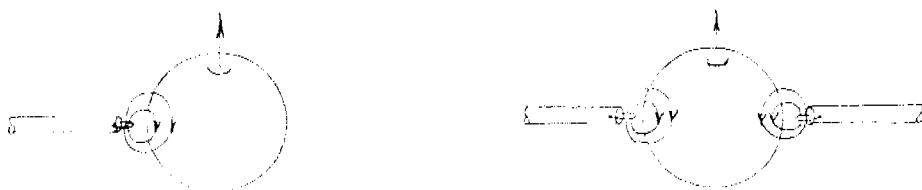
product of signal height and linewidth is constant under conditions of no (or weak) saturation.] Now  $M \propto S^2 / 5$ , a factor of 100 improvement over  $M_0$ . Thus a quadratic gain in  $M$  results from a decrease in linewidth.

If we reduce the Rb density by a factor of 100, the signal drops by this same factor to  $S^2 / 100$ , assuming constant linewidth. But now  $M = M_0 \propto S^2 / 500$ . Thus the same  $M$  is achieved with 1/100 the original Rb density. In gas cells as used in Rb frequency standards, 500-700 Hz are typical linewidths. A sizable fraction of this linewidth is due to Rb - Rb spin exchange collisions due to the high required Rb density. The simple argument presented above shows that operation of the EWSC is feasible at Rb densities far less than those used in gas cells. Hence, Rb-Rb collisional broadening due to spin exchange need not be a major component in the linewidth of evacuated wall-coated cells even when operated at a figure of merit comparable to or exceeding that of gas cells.

#### EXPERIMENTAL TECHNIQUE

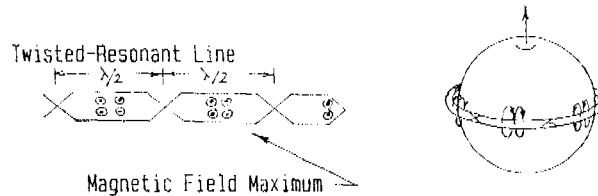
The attainment of a large spike-to-pedestal signal ratio can proceed in two stages: minimizing the spike linewidth and maximizing the  $\langle B_1^2 \rangle / \langle B_1 \rangle$  ratio. Among the factors determining the spike linewidth are dispersion in phase shift at wall (dominant cause of intrinsic width): light intensity broadening: microwave power broadening: geometric lifetime: etc. The phase shift component of width is proportional to  $1/R$  where  $R$  is a measure of cell size. In [1], using a cell with a diameter to  $\lambda/2$  ratio of 3.3, a 12:1 spike-to-pedestal height ratio was attained by judicious adjustment of a microwave horn's location/orientation with respect to the cell. A second method was also used to achieve the  $\langle B_1 \rangle \neq 0$  condition.

In this case a small microwave loop whose dimensions were comparable to  $\lambda/20$  was positioned close to the cell wall with appropriate orientation to provide a sizable fraction of its field with proper orientation to drive the desired hyperfine transition. The spatial phase of the near-zone field does indeed change phase at a  $\lambda/2$  distance from the loop: but the spatial gradient in the microwave field due to the small loop size reduces the amplitude of the unwanted phase so that  $\langle B_1 \rangle \neq 0$  as desired. See sketch.



The result is that an atom samples the field at random times but remains phased with the inducing field's phase even when so far away as to see no field. On each entrance into the field it continues making a transition. Thus the spike feature is large. The pedestal is also present although its lineshape is altered from Gaussian. One linewidth contribution to the pedestal is now due to the lifetime the atom spends in one pass through the localized field. (Lineshape due solely to the lifetime effect would be Lorentzian.) Since the ensemble has a velocity distribution, this width is weighted by this distribution. Deviations from Gaussian pedestal lineshape were observed. Effects of the far and intermediate zone fields have been calculated for  $\langle B_1^2 \rangle$  and  $\langle B_1 \rangle$  as a function of cell size.

A symmetric array of dipoles can also be used. A pair are sketched above. An extension of the array is a resonant-line structure constructed in principle of twisted sections each of length  $\lambda/2$ .



Quadrupole loops have been used to create even stronger spatial gradient field falloffs. Unwanted microwave fields can be controlled by appropriately placed absorptive material.

Larger cell size is advantageous in providing smaller linewidth and increasing the signal at constant Rb density. Not only is signal increased because linewidth is decreased, but also since a larger number of Rb atoms are being interrogated (assuming constant Rb density). However, it may then become more difficult to attain a reasonable  $\langle B_z^2 \rangle / \langle B_1^2 \rangle$  ratio. Likewise, in using smaller cells of interest in miniaturization, a microwave cavity mode may be selected in which  $\langle B_1^2 \rangle = 0$ , thus producing no spike signature at all. An example of this is the wall-coated cell which fills a TE111 mode cavity.[6] Use of such modes is still possible by physically dividing the cell with a septum placed along the region where the spatial phase changes, although the smaller effective cell size will increase spike linewidth. In fact for the hydrogen maser, this has been proposed.[11]

#### PRACTICAL CONSIDERATIONS

Consider use of an EWSC in a TE011 mode cavity. In a right-circular non-loaded cavity, the spatial average of the z-component of the cavity magnetic field over a spherical cell is given by

$$\langle B_z^2 \rangle / B_{\text{center}}^2 = 3 \left[ \frac{\sin \Omega}{\Omega^3} - \frac{\cos \Omega}{\Omega^2} \right]$$

with  $\Omega = (R_{\text{cell}}/D_{\text{cavity}}) \times [(kD)^2 + \pi^2]^{1/2}$  :  $kD = 2 \times 3.832$   
In the hydrogen maser, the filling factor given below is a relevant parameter.

$$\eta_H = \langle B_z^2 \rangle_{\text{cell}} / \langle B_{\text{tot}}^2 \rangle_{\text{cavity}}$$

$$\text{with } \langle B_{\text{tot}}^2 \rangle_{\text{cavity}} / B_{\text{center}}^2 = J_0^2(kR_{\text{cav}}) \times [1 + (\pi/kL)^2]/2$$

where L = cavity length and R<sub>cav</sub> = cavity radius. A closed form expression for  $\eta_H$  is thus found. This is plotted in Fig. 1. This result does not agree with KGR's[5] Fig. 3 (corrected by a factor of two) when the cell radius is large. It appears that KGR may have plotted  $\langle B_z^2 \rangle_{\text{cell}} / \langle B_{\text{tot}}^2 \rangle_{\text{cav}}$ .

A plot of the 'filling factor' for the EWSC,  $\langle B_z^2 \rangle_{\text{cell}} / \langle B_{\text{tot}}^2 \rangle_{\text{cavity}}$ , is given in Fig. 2. This is the relevant quantity for field averages when driving the (2,0) - (1,0) hyperfine transition. Rho,  $\rho$ , is the cell radius/cavity diameter. First results on a cell  $\sim 30$  cc give an intrinsic linewidth of  $\sim$

20 Hz at 6.8 GHz with 1.5  $\mu$ A light intensity. The hfs resonance in this cell is shown in Fig. 3.

## CONCLUSIONS

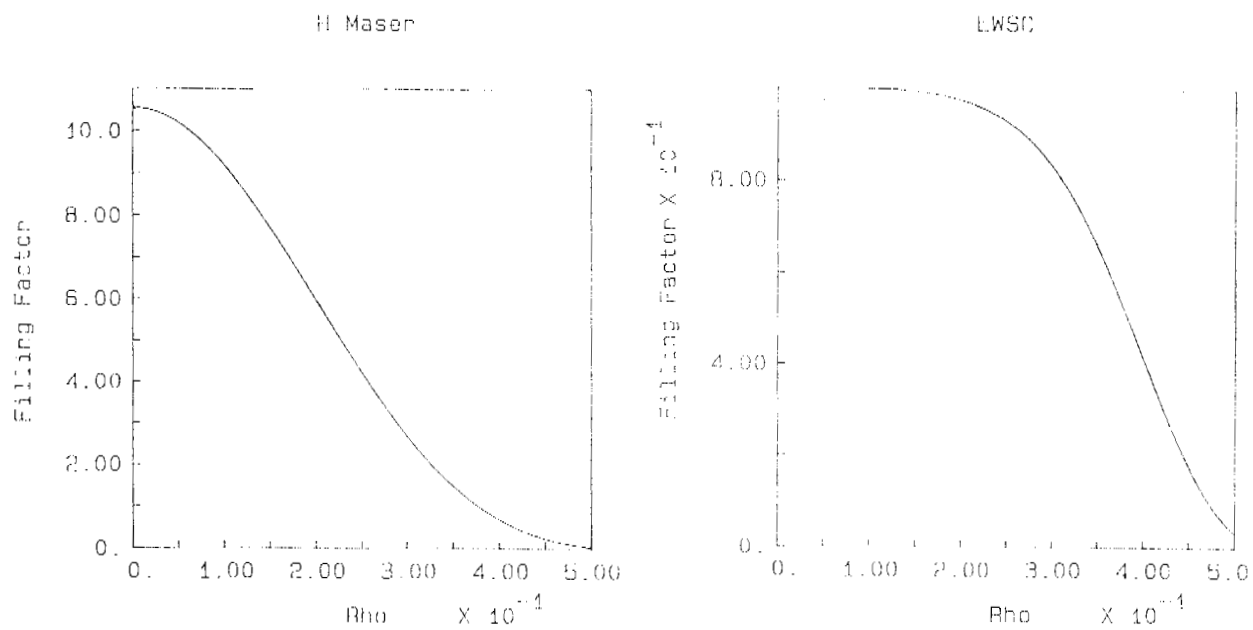
As a practical matter, it appears that large EWSC,  $D > \lambda$ , are not necessary to attain significant figures of merit. A cell which fits in TE011 mode cavity is a good example. The EWSC appears to remain an excellent candidate for atomic frequency standard use.

## ACKNOWLEDGEMENT

Work supported in part by the Duke University Research Council.

## REFERENCES

1. H.G. Robinson and C.E. Johnson, *Appl. Phys. Lett.* **40**, 771(1982).
2. H.G. Robinson and C.E. Johnson, *Proc. 14th PTTI*, 307(1982).
3. H.G. Robinson and C.E. Johnson, *IEEE Trans. Inst. Meas.* **IM-32**, 198(1983).
4. R.H. Dicke, *Phys. Rev.* **89**, 472(1953); R.H. Romer and R.H. Dicke, *Phys. Rev.* **99**, 532(1955).
5. D. Kleppner, H.M. Goldenberg, and N.F. Ramsey, *Phys. Rev.* **126**, 603(1962).
6. R.P. Frueholz, C.H. Voit, and J.C. Camparo, *J. Appl. Phys.* **54**, 5613(1983).
7. R.P. Frueholz and C.H. Voit, *Proc. 38th Annual Freq. Control Symp.*, 401(1984).
8. S.F. Watanabe and H.G. Robinson, *J. Phys. B: Atom. Molec. Phys.*, **10**, 931(1977).  
S.F. Watanabe, G.S. Bayne, and H.G. Robinson, *ibid.*, 941.  
S.F. Watanabe and H.G. Robinson, *ibid.*, 959.  
J. Sykes, *ibid.*, 1151.  
S.F. Watanabe and H.G. Robinson, *ibid.*, 1167.
9. S.B. Crampton, E.C. Flory, and H.T.M. Wang, *Metrologia* **13**, 131(1977).
10. Compare with reference 7 in which the authors attribute to Vanier et al. [J. Vanier, J.F. Simard, and J.R. Boisjanger, *Phys. Rev. A9*, 1031(1974)] the idea that the mechanism of wall collisions and gas collisions are identical insofar as concerns the colliding Rb atom.
11. E.M. MacCison, M.W. Levine, R.F.C. Vessot, *Proc. 8th PTTI Meeting*, 355(1976).



Figures 1 & 2. The filling factors for the H-maser,  $\langle B_z \rangle_{\text{cell}}^2 / \langle B_{\text{tot}} \rangle_{\text{cavity}}$ , and for the EWSC used with optical pumping,  $\langle B_z \rangle_{\text{cell}}^2 / \langle B_z^2 \rangle_{\text{cell}}$ , in an unloaded cylindrical right-circular TE011 mode cavity. Rho is  $R_{\text{cell}} / D_{\text{cavity}}$ .

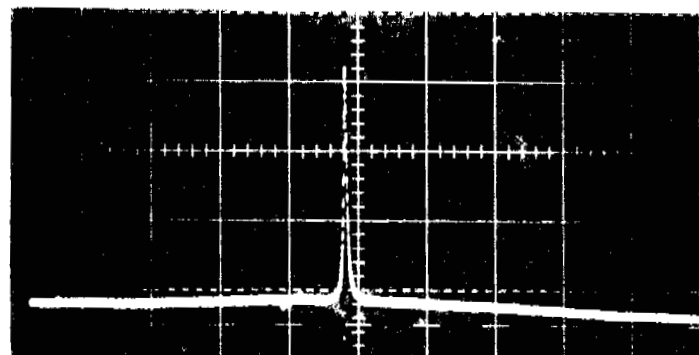


Figure 3. The 0-0 hyperfine transition resonance in a 30 cc cell shown with a wide sweep.

## QUESTIONS AND ANSWERS

HARRY PETERS, SIGMA TAU CORPORATION: I was curious as to what your wall coating was, and what the stability of frequency, or linewidth would be.

MR. ROBINSON: This particular coating is the same coating we used originally. It's Tetracontane. Time is the main thing that prevents us from trying other coatings. We would give the same answer to your second question. We really haven't explored in detail how stable the frequency is, or the linewidth and so forth. Those are things that clearly need to be done. The talk this afternoon right after lunch details some of the parameters that are important in deciding whether you can use this for atomic frequency standards. That particular issue is not addressed, though, this afternoon.